PAPER

Harmonics analysis of the ITER poloidal field converter based on a piecewise method

Plasma Sci. Technol. **19** (2017) 125602 (8pp) https://doi.org/10.1088/2058-6272/aa86a5

Harmonics analysis of the ITER poloidal field converter based on a piecewise method

Xudong WANG (王旭东)[1,2], **Liuwei XU** (许留伟)[1,4], **Peng FU** (傅鹏)[1,2], **Ji LI** (李冀)[3] **and Yanan WU** (吴亚楠)[1]

[1] Institute of Plasma Physics, Chinese Academy of Science, Hefei 230031, People's Republic of China
[2] University of Science and Technology of China, Hefei 230026, People's Republic of China
[3] Maintenance Company, State Grid Anhui Electric Power Company, Hefei 230061, People's Republic of China

E-mail: xulw@ipp.cas.cn

Received 31 May 2017, revised 14 August 2017
Accepted for publication 16 August 2017
Published 23 October 2017

Abstract

Poloidal field (PF) converters provide controlled DC voltage and current to PF coils. The many harmonics generated by the PF converter flow into the power grid and seriously affect power systems and electric equipment. Due to the complexity of the system, the traditional integral operation in Fourier analysis is complicated and inaccurate. This paper presents a piecewise method to calculate the harmonics of the ITER PF converter. The relationship between the grid input current and the DC output current of the ITER PF converter is deduced. The grid current is decomposed into the sum of some simple functions. By calculating simple function harmonics based on the piecewise method, the harmonics of the PF converter under different operation modes are obtained. In order to examine the validity of the method, a simulation model is established based on Matlab/Simulink and a relevant experiment is implemented in the ITER PF integration test platform. Comparative results are given. The calculated results are found to be consistent with simulation and experiment. The piecewise method is proved correct and valid for calculating the system harmonics.

Keywords: harmonics, PF converter, piecewise method

(Some figures may appear in colour only in the online journal)

1. Introduction

The magnet system is a core part of a tokamak fusion reactor. The AC/DC magnet power converter provides a controlled DC voltage and current to the magnet coils. The magnet coils are able to carry high current and produce strong magnetic fields. At present, the magnet power converters mainly utilize thyristor technology in addition to the ITER poloidal field (PF) converter. The ITER PF converter consists of four six-pulse thyristor bridges, supplied by two phase-shifted transformers. It is decoupled by external inductors and achieves four-quadrant operation [1]. The ITER PF integration test platform was built to demonstrate the feasibility of this scheme [2, 3].

Thyristor phase-control technology results in a large number of harmonics. Harmonics is related to filter design, grid security and electrical equipment safety [4–8]. It is one of the most important and difficult research areas in a converter system. The traditional method is to integrate complex trigonometrical functions within their repetition period [9–11]. However, as it operates in three modes, the harmonics of the PF converter is more complicated than a single six-pulse converter unit. Traditional integral operation in Fourier analysis is complicated and inaccurate. A method for Fourier coefficient calculations has been proposed. The method was described wherein algebraic addition is substituted for integration, which is analogous to the Laplace operator method where the algebraic operation is substituted for differentiation and integration [12–14].

According to the operation principle of the PF converter, this paper processes the expression of the system grid current. The grid current is decomposed into the sum of some simple functions. Each simple function harmonics can be calculated separately, which is analogous to the Laplace operator method [14, 15]. By applying this approach, this paper presents a

[4] Author to whom any correspondence should be addressed.

piecewise method to calculate the characteristic harmonics in three different operation modes of the PF converter. The PF converter model is established based on Matlab/Simulink. The model harmonics analysis is done using a Simulink FFT analysis tool. The relevant experiment is implemented in the ITER PF integration test platform. The grid current in three different operation modes are analyzed using a power quality analyzer. The simulation and experimental results are given to verify the validity of the piecewise method.

In this paper, the theoretical analysis on harmonics is based on the assumptions below.

1. Grid voltages are assumed as ideal symmetric three-phase voltage sources, and distortion of grid voltage is neglected.
2. As the dummy load is a large inductance, the DC output current is completely filtered without AC components.
3. Losses in bridge inductance are neglected.
4. The step-down and converter transformers excitation currents are ignored.

2. The ITER PF converter system

2.1. Operation analysis

The topology of a basic unit for the ITER PF converter is shown in figure 1. The system obtains energy from a 110 kV power grid. The step-down transformer transforms the voltage of the power grid to 66 kV to supply two phase-shifted converter transformers T2 and T3. The two converter transformers supply ±15° phase-shifted voltages by extended delta primary. Converter unit 1 (CU1) and CU2 are connected in anti-parallel, supplied by T2. CU3 and CU4 are anti-parallel and supplied by T3. Four six-pulse bridges CU1–CU4 are decoupled by external inductors L1–L4, respectively. The PF converter can work in four-quadrant operation with an output current up to ±55 kA. The main parameters of the system are listed in table 1.

There are three operation modes, the circulating mode, single mode and parallel mode, as shown in figure 2. The circulating mode is designed to achieve current polarity change smoothly. When the PF converter operates in a low current level (<18% rated current I_{dn}), CU1 outputs current I_{d1}, which establishes a circulating current with I_{d4} supplied by anti-parallel CU4. When $0.18I_{dn} < |I_d| < 0.36I_{dn}$, only CU1 or CU4 works in single mode. When it needs to output a large current ($|I_d| > 0.36I_{dn}$), the PF converter operates in parallel mode with two converter bridges in the same direction. The specific working sections are shown in figure 2.

According to the system operation, the equivalent circuit of each mode is shown in figure 3. As phase-control technology is adopted in the converter bridge, the mathematical formulas are derived easily based on Kirchhoff's laws, as listed in equation groups (1) and (2). The parameters are listed below:

α_1–α_4: firing angles of CU1–CU4;
L: dummy load inductance;

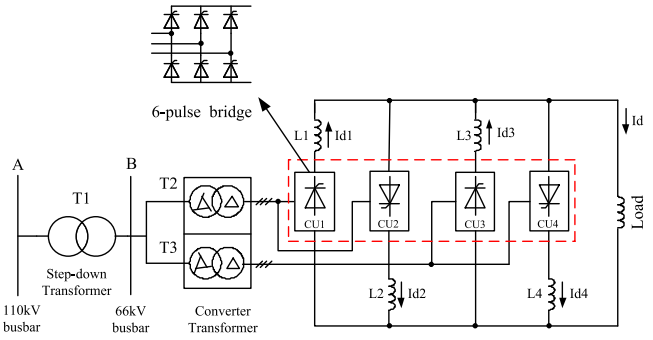

Figure 1. ITER PF converter topology.

R_d: dummy load resistance;
L_r: DC reactor inductance;
R_r: DC reactor resistance;
R_s: system equivalent resistance, mainly including transformer short circuit impedance;
U_1–U_4: output on-load voltages of CU1–CU4;
γ: bridge commutation angle;
X_B: equivalent grid reactance, mainly including transformer reactance.

Circulating mode:

$$\begin{cases} 1.35U_{ab}\cos\alpha_1 - (R_s + R_r)i_{d1} = L_r\dfrac{di_{d1}}{dt} + L\dfrac{di_d}{dt} + R_d i_d \\ 1.35U_{ab}\cos\alpha_4 + (R_s + R_r)i_{d4} = -L_r\dfrac{di_{d1}}{dt} + L\dfrac{di_d}{dt} + R_d i_d \\ i_c = i_{d4} = i_{d1} - i_d \end{cases} \tag{1-a}$$

Single mode:

$$1.35U_{ab}\cos\alpha_1 - (R_s + R_r)i_d = (L + L_r)\frac{di_d}{dt} + R_d i_d. \tag{1-b}$$

Parallel mode:

$$\begin{cases} 1.35U_{ab}\cos\alpha_1 - (R_s + R_r)i_{d1} = L_r\dfrac{di_{d1}}{dt} + L\dfrac{di_d}{dt} + R_d i_d \\ 1.35U_{ab}\cos\alpha_3 - (R_s + R_r)i_{d3} = L_r\dfrac{di_{d3}}{dt} + L\dfrac{di_d}{dt} + R_d i_d \\ i_{d1} = i_{d3} = \dfrac{1}{2}i_d \end{cases} \tag{1-c}$$

$$\cos\alpha - \cos(\alpha + \gamma) = \frac{2X_B I_d}{\sqrt{2}\,U_{ab}}. \tag{2}$$

Through the above calculations, the firing angle α and commutation angle γ can be figured out under different operation modes. These parameters are used in the harmonics analysis, which is described in detail in the next section 3.

2.2. Analysis of current characteristics

According to the equivalent circuit of the clockwise extended-delta connection converter transformer shown in figure 4, its

Table 1. Parameters of the ITER PF converter.

	Parameter	Value
Step-down transformer	Rated power, MVA	100
	Short circuit impedance	9.48%
	Rated primary/secondary voltage, kV	110/66
	Rated power, MVA	2 × 41
	Short circuit impedance	16%
Converter transformer	Rated primary/secondary voltage, kV	66/1.05
	Connection group primary/secondary	Phase shifting ±15°, extended-delta/delta
	DC reactor	200 μH/300 $\mu\Omega$
	Dummy load	5 mH /3 mΩ
	On-load output voltage, kV	±1.05
	Output current, kA	±55

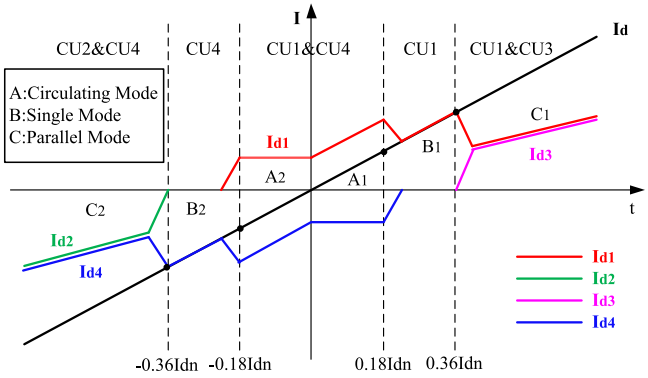

Figure 2. ITER PF converter operation modes.

voltage vector diagram is made, as shown in figure 5. Depending on the voltage vector diagram, some equations related to the transformer are derived, as shown in the following:

$$k_1 + k_2 = 1 \tag{3}$$

$$k_1 = \frac{\sin(30^\circ - \varphi)}{\sin(30^\circ + \varphi)} \tag{4}$$

$$n = k \times \frac{\sin(30^\circ + \varphi)}{\sin 120^\circ} \tag{5}$$

where: k: voltage ratio of the transformer;

k_1: primary extended winding coefficient;
k_2: primary delta winding coefficient;
n: turns ratio of the transformer;
φ: phase-shifted angle 15°.

While extended-delta winding is utilized in the converter transformer to shift the phase to 15°, electromagnetic equation group (6) can be derived using the magnetic potential balance principle. In equation group (6), the transformer excitation current is ignored. The various components are shown in the following:

I_{A1}, I_{B1} and I_{C1}: primary extended winding current
I_{A2}, I_{B2} and I_{C2}: primary delta winding current;
I_{ca}, I_{ab} and I_{bc}: secondary winding current;
I_a, I_b and I_c: secondary line current;
W_1: primary extended winding;
W_2: primary delta winding;

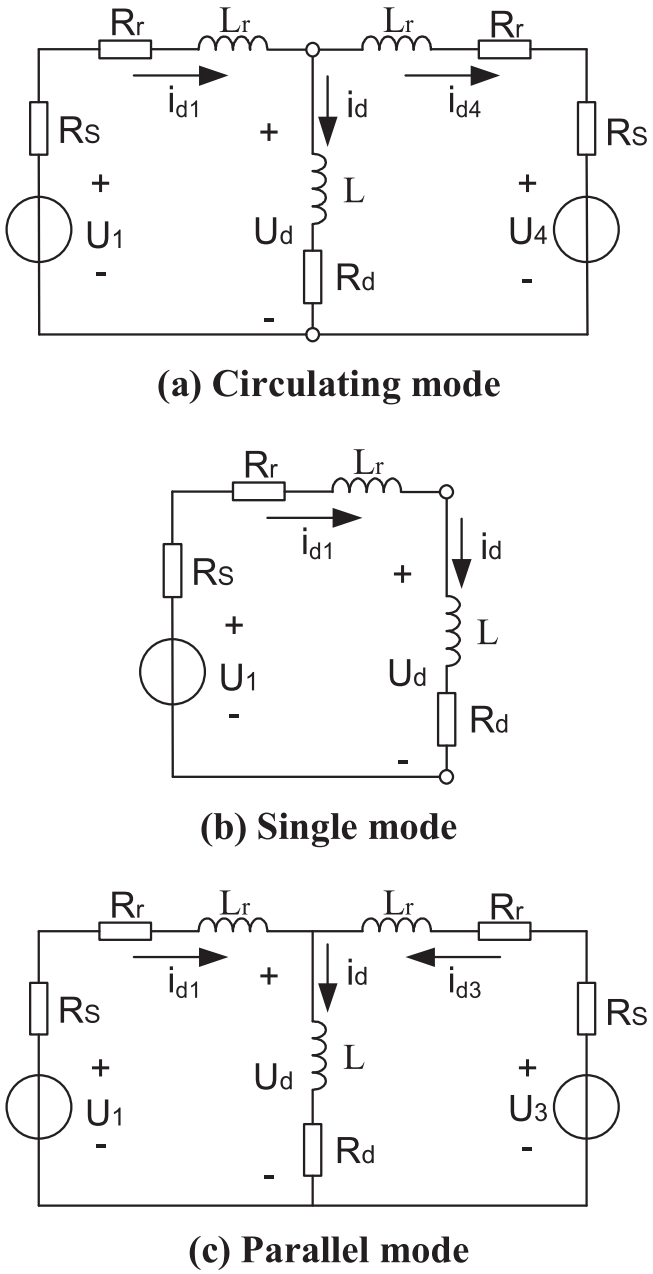

Figure 3. Equivalent circuit diagrams of the PF converter.

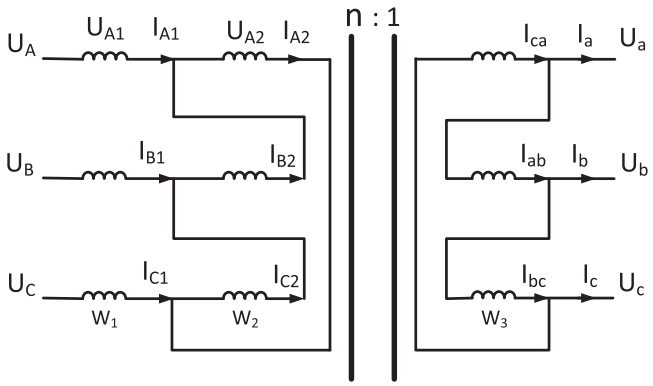

Figure 4. Equivalent circuit of the clockwise extended-delta connection converter transformer.

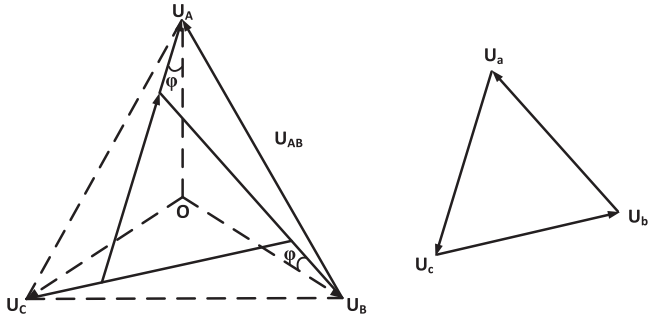

Figure 5. Voltage vector diagram of the clockwise extended-delta connection converter transformer.

W_3: secondary winding.

$$\begin{cases} W_1 I_{A1} + W_2 I_{A2} - W_3 I_{ca} = 0 \\ W_1 I_{B1} + W_2 I_{B2} - W_3 I_{ab} = 0 \\ W_1 I_{C1} + W_2 I_{C2} - W_3 I_{bc} = 0 \end{cases} \tag{6}$$

$$\begin{cases} I_a = I_{ca} - I_{ab} \\ I_b = I_{ab} - I_{bc} \\ I_c = I_{bc} - I_{ca} \\ I_a + I_b + I_c = 0 \\ I_{ca} + I_{ab} + I_{bc} = 0 \end{cases} \Rightarrow \begin{cases} I_{ab} = \dfrac{1}{3}(I_b - I_a) \\ I_{bc} = \dfrac{1}{3}(I_c - I_b) \\ I_{ca} = \dfrac{1}{3}(I_a - I_c) \end{cases} \tag{7}$$

$$\begin{cases} I_{A1} = I_{A2} - I_{B2} \\ I_{B1} = I_{B2} - I_{C2} \\ I_{C1} = I_{C2} - I_{A2} \\ I_{A1} + I_{B1} + I_{C1} = 0 \\ I_{A2} + I_{B2} + I_{C2} = 0 \end{cases} \Rightarrow \begin{cases} I_{A2} = \dfrac{1}{3}(I_{A1} - I_{C1}) \\ I_{B2} = \dfrac{1}{3}(I_{B1} - I_{A1}) \\ I_{C2} = \dfrac{1}{3}(I_{C1} - I_{B1}) \end{cases} \tag{8}$$

$$\begin{bmatrix} I_{A1} \\ I_{B1} \\ I_{C1} \end{bmatrix} = m \begin{bmatrix} k_1 + k_2 & 0 & -k_1 \\ -k_1 & k_1 + k_2 & 0 \\ 0 & -k_1 & k_1 + k_2 \end{bmatrix} \begin{bmatrix} I_a \\ I_b \\ I_c \end{bmatrix} \tag{9}$$

where $m = \dfrac{1}{3nk_1^2 + 3nk_1k_2 + nk_2^2}$; $W_1/W_3 = nk_1$; $W_2/W_3 = nk_1$.

Secondary winding currents are expressed by secondary line currents, and primary delta winding currents are expressed by primary line currents. Substituting the derivative results of equation groups (7) and (8) into equation group (6), the primary line currents can be derived, as shown in equation (9).

The anticlockwise extended-delta connection converter transformer is similar to the clockwise one. Its voltage vector lags behind the clockwise one. Primary current equation group expressed by the secondary line current is listed in equation (10).

$$\begin{bmatrix} I_{A1} \\ I_{B1} \\ I_{C1} \end{bmatrix} = m \begin{bmatrix} k_1 + k_2 & -k_1 & 0 \\ 0 & k_1 + k_2 & -k_1 \\ -k_1 & 0 & k_1 + k_2 \end{bmatrix} \begin{bmatrix} I_a \\ I_b \\ I_c \end{bmatrix}. \tag{10}$$

This section presents the system operation principle. According to the circuit topology and the principle of a phase shifting transformer, the primary current is derived, which is expressed by a secondary current. The relationship between the primary and secondary currents is used to calculate harmonics that are injected into power grid. The detailed calculation method is discussed in the next theoretical analysis section 3.

3. Theoretical harmonics analysis

According to the Biringer formula, the harmonics can be calculated using the jumps in the function at the points of discontinuity. The Fourier coefficients of the constant function are determined by equation (11). As shown in equation (12), Fourier coefficients of the sine function are determined by both the function and its derivative jumps at the points of the function discontinuities [12].

$$\phi_n = \frac{2}{\mathrm{j}k^*T} \sum_{i=1}^{n} \delta_i \mathrm{e}^{-\mathrm{j}k^*t_i} \tag{11}$$

$$\phi_n = \frac{2}{\mathrm{j}(1 - k^{*2})} \sum_{i=1}^{n} (\mathrm{j}k^*\delta + \delta_i')\mathrm{e}^{-\mathrm{j}k^*t_i}. \tag{12}$$

Here $\delta_i = f(t_i + 0) - f(t_i - 0)$ is the value of the jump of the function at the general point t_i;

δ_i' is a derivative of δ_i;
$k^* = k(2\pi/t)$ is the order of the harmonics of the waveform with respect to k;
$k = 0, 1, 2, \ldots$;
ϕ_n is amplitude of the harmonic.

Referring to [13], the secondary line current of the converter transformer is decomposed into a rectangular component and a sine component, as shown in figure 6. For each simple waveform, their harmonics can be calculated by equations (11) and (12), respectively. The Fourier coefficient of each waveform can be synthesized for the same order. Thus the harmonics of each converter transformer secondary line current can be calculated using this piecewise method. Equation (13) shown below is the secondary harmonic current of the clockwise converter transformer.

$$I_{a1k} = 2\sqrt{3} I \mathrm{e}^{-\mathrm{j}k\alpha} \mathrm{e}^{\pm \mathrm{j}\frac{\pi}{6}} \times \left[\frac{\cos\alpha + \mathrm{j}k\sin\alpha - [\cos(\alpha + \gamma) + \mathrm{j}k\sin(\alpha + \gamma)]\mathrm{e}^{-\mathrm{j}k\gamma}}{\mathrm{j}k(1 - k^2)\pi} \right] \tag{13}$$

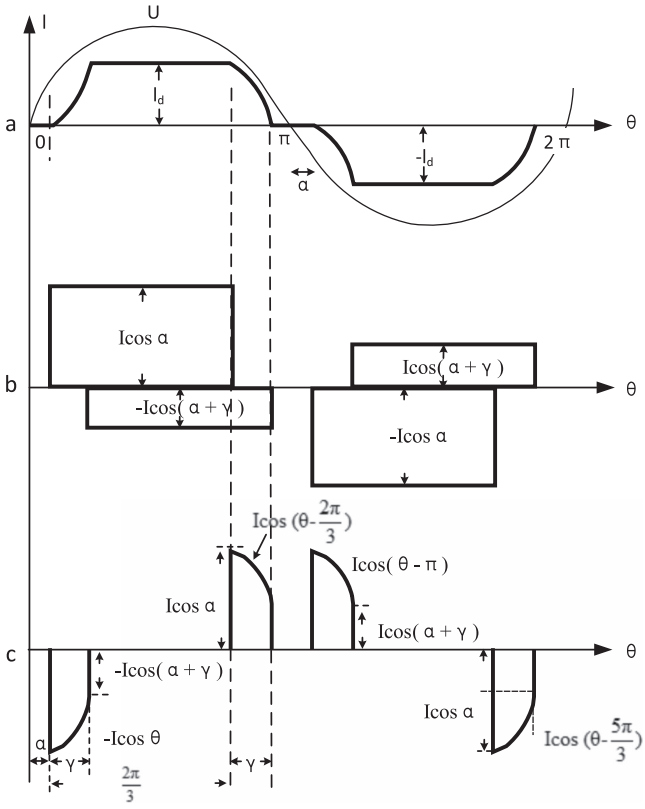

Figure 6. Secondary line current of the transformer. (a) General form. (b) Constant component. (c) Sine component.

$$\text{where: } e^{\pm j\frac{\pi}{6}} = \begin{cases} e^{+j\frac{\pi}{6}} & k = 6\nu + 1, \quad \nu = 0, 1, 2, \cdots \\ e^{-j\frac{\pi}{6}} & k = 6\nu - 1, \quad \nu = 0, 1, 2, \cdots \end{cases}$$

$$I = I_{dT2} \times \frac{1}{\cos\alpha - \cos(\alpha + \gamma)}.$$

I_{dT2} is the DC output current powered by clockwise converter transformer T2. I_{dT2} equals I_{d1} or I_{d2} depending on whether CU1 or CU2 is at work.

There are only harmonics in order $k = 6\nu \pm 1$, $\nu = 1$, 2, …, and all other harmonics are zero. According to the analysis in section 2, the secondary current based on the anticlockwise extended-delta connection lags behind the clockwise one by 30 electrical degrees. Therefore, the other phase harmonic currents can be calculated by phase shifting with the same harmonic order, as shown in equation group (14).

$$\begin{cases} I_{b1k} = I_{a1k} \cdot e^{-jk\frac{2\pi}{3}} \\ I_{c1k} = I_{a1k} \cdot e^{jk\frac{2\pi}{3}} \\ I_{a2k} = \dfrac{I_{dT3}}{I_{dT2}} \cdot I_{a1k} \cdot e^{-jk\frac{\pi}{6}} \\ I_{b2k} = \dfrac{I_{dT3}}{I_{dT2}} \cdot I_{a1k} \cdot e^{-jk\frac{\pi}{6}} e^{-jk\frac{2\pi}{3}} \\ I_{c2k} = \dfrac{I_{dT3}}{I_{dT2}} \cdot I_{a1k} \cdot e^{-jk\frac{\pi}{6}} e^{jk\frac{2\pi}{3}} \end{cases} \quad (14)$$

where I_{dT3} is the DC output current powered by anticlockwise converter transformer T3. I_{dT3} equals I_{d3} or I_{d4} depending on whether CU3 or CU4 is at work.

I_{a1k}, I_{b1k} and I_{c1k} are the clockwise converter transformer secondary kth harmonic currents.

I_{a2k}, I_{b2k} and I_{c2k} are the anticlockwise converter transformer secondary kth harmonic currents.

Referring to the analysis of current characteristics in section 2, the primary current is expressed by an algebraic sum of the secondary current. The essence of the piecewise method is to split equations into the sum of some simple functions to calculate the harmonics individually. Therefore, the primary harmonic current is equal to the algebraic sum of the secondary harmonic current. It only takes putting secondary harmonic currents into equations (9) and (10). Taking phase A of the transformer as an example, the primary harmonic currents are derived below. Equations (15) and (16) are based on clockwise and anticlockwise transformers, respectively.

$$I_{A1k} = m[(k_1 + k_2)I_{a1k} - k_1 I_{c1k}] \quad (15)$$

$$I_{A2k} = m[(k_1 + k_2)I_{a2k} - k_1 I_{b2k}]. \quad (16)$$

I_{A1k} and I_{A2k} are the harmonics produced by one converter transformer individually. For the total harmonics in the power grid, we need to add up the same order primary harmonics produced by two converter transformers, $I_{Ak} = I_{A1k} + I_{A2k}$. So far, the harmonics produced by the PF converter system have been figured out based on the piecewise method.

In summary, the piecewise method discretizes the complex secondary current. For each simple waveform, the Fourier coefficient can be calculated easily and they are used as elements. The Fourier coefficients depend only on the jumps of the function components and on their derivatives. The determination of these jumps is very simple. Depending on the operation modes, the Fourier coefficient of a simple waveform can be synthesized. According to the relationship between the primary and secondary current, the harmonics can be figured out in the grid side.

4. Simulation modeling and experiment verification

4.1. Simulation modeling

The PF converter is modeled based on Matlab/Simulink. The parameters of the model are consistent with the actual PF converter platform. Figure 7 shows a diagram of the model. Four-quadrant operation of the PF converter model is shown in figure 8. As it is presented, the simulated output current I_d accords with the preset I_d (green I_d overlaps with the black preset I_d). CU1–CU4 are well operated in three modes. The circulating I_c is set to 7.5 kA. The maximum output current is the rated current ±55 kA. The whole operation time is 30 s [15–17].

4.2. Experiment verification

In order to verify the correctness of the theoretical calculation and simulation results, an experiment using the PF converter was carried out under the same conditions. The ITER PF

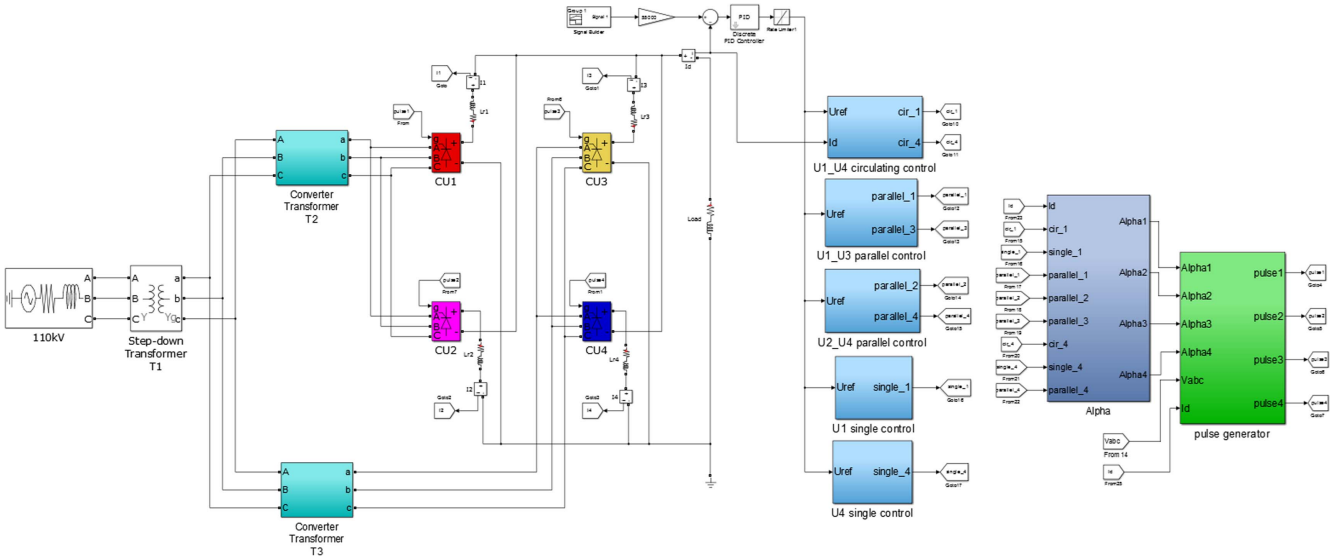

Figure 7. Full diagram of the PF converter Simulink model. (CU1: red; CU2: magenta; CU3: yellow; CU4: blue.).

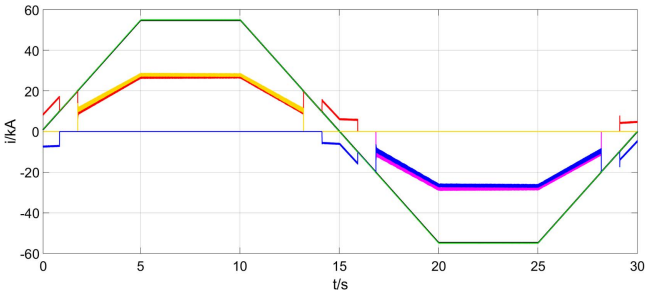

Figure 8. Four-quadrant operation of the PF converter model. (I_{d1}: red; I_{d2}: magenta; I_{d3}: yellow; I_{d4}: blue; I_d: green; preset I_d: black.).

integration test platform is shown in figure 9. The experiment was designed for the same four-quandrant operation under the same parameter settings as presented in section 4.1.

Comparing simulation with the experiment results shown in figure 10, both of them realize four-quadrant operation and CU1–CU4 work in three modes very well. The accuracy and linearity of the control system are very good. So it is suitable for verifying the calculation method by comparing with simulation and experiment.

Apparently it has different harmonic performance in three operation modes. Therefore, it is necessary to carry out a harmonics analysis. In this paper we selected three time nodes to analyze its harmonics under three operation modes individually. The selected time nodes and output currents are listed in table 2. Setting the system startup as time zero.

The theoretical values can be calculated using the piecewise method discussed in the previous sections. Compared with the fundamental period of grid current, $\mathrm{d}i_d/\mathrm{d}t$ of the output current is small. Ten fundamental cycles of the grid current after the time node are chosen to calculate the average current, which is used in the theoretical calculation. The simulation harmonics of the model can be obtained by the FFT analysis tool easily in Matlab/Simulink. The same number of fundamental cycle after the time node is put in the FFT window to the analyze harmonics. The 110 kV grid

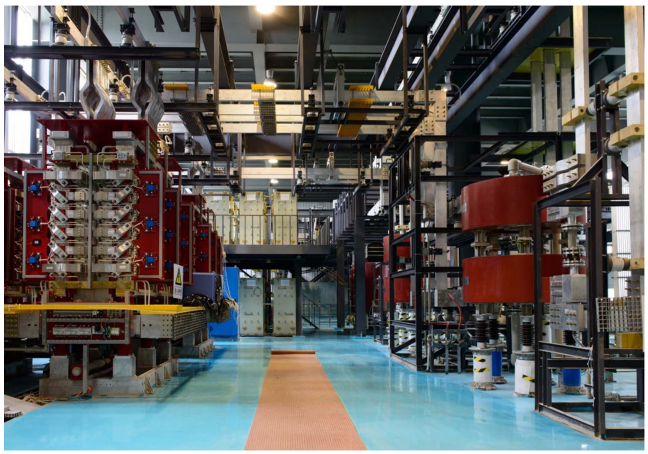

Figure 9. The ITER PF integration test platform.

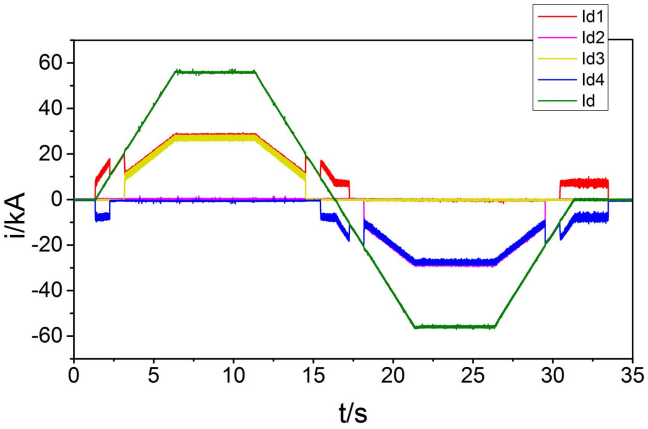

Figure 10. Four-quadrant operation of the PF platform experiment (I_{d1}: red; I_{d2}: magenta; I_{d3}: yellow; I_{d4}: blue; I_d: green.).

current in the same time nodes is analyzed using a power quality analyzer in the experiment. It also analyzes ten fundamental cycles. All three kinds of results are converted to 110 kV grid side.

Table 2. The selected time nodes with operation modes.

Mode	Time (s)	I_{d1} (kA)	I_{d2} (kA)	I_{d3} (kA)	I_{d4} (kA)	I_d (kA)
Circulating	0.68	15	—	—	7.5	7.5
Single	1.48	16.3	—	—	—	16.3
Parallel	6	27.5	—	27.5	—	55

Table 3. Comparisons of harmonics amplitude in 110 kV grid (unit: A).

Mode	Harmonic order	5th	7th	11th	13th	17th	19th
Circulating	Calculation	15.6	10.71	12.13	8.34	5.74	5.08
	Simulation	16.6	10.07	12.84	8	6.8	5.74
	Experiment	16.5	10	13.5	8.6	5.1	3.8
Single	Calculation	24.15	16.82	9.9	7.96	5.3	4.36
	Simulation	24.85	16.85	10.3	8.07	5.62	4.56
	Experiment	24.9	17.1	10.6	8.3	5.8	4.3
Parallel	Calculation	1.7	1	25.85	19	0.44	0.33
	Simulation	1.37	0.7	25.45	19.8	0.12	0.23
	Experiment	2.5	3.5	24.4	15.1	1.1	1.1

5. Comparison and analysis of results

The experimental results compared with the simulation FFT analysis and the theoretical calculation are listed in table 3. It is important to note that two branch currents are equal in ideal parallel mode. There are only harmonics in order $k = 12\nu \pm 1$, $\nu = 1, 2, \ldots$. To calculate the harmonics exactly in parallel mode, a current error is added between two branch currents in the theoretical analysis, which is set at 0.5 kA, depending on the actual experimental error. The higher 19th harmonics are so small that they are negligible.

The harmonics histograms of calculation, simulation and experiment are shown in figure 11. Through the comparison of the results, it can be seen that the theoretical values of the characteristic 5th, 7th, 11th, 13th, 17th and 19th harmonics are basically equal to the simulation and experimental results. The theoretical analysis is consistent with simulation and experiment in three modes.

In the single mode, the calculation values are the most accurate because there is only one converter unit at work. Compared with the other two modes, which have two converter units at work all the time, the single mode is simpler and it has no coupling problems. In some harmonics orders, the experimental results have slight differences to the calculation and simulation. In practice, it is impossible to have two identical converter units. In addition, the parasitic parameters in experiment cannot be measured exactly. The non-linearity of reactors and distortion of line voltages may cause some non-characteristic harmonics. These are reasons for the deviation between the theory and practice [17].

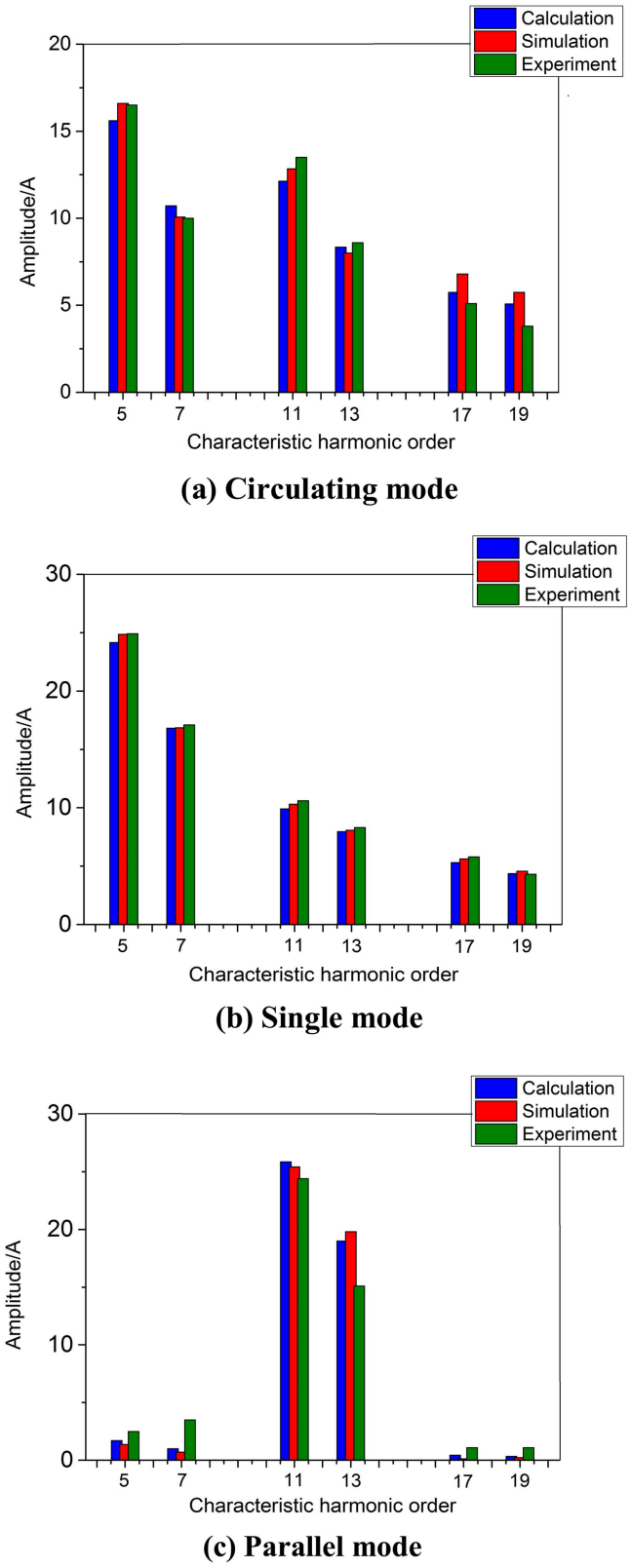

Figure 11. Harmonics histograms of calculation, simulation and experiment.

Above all, the piecewise method is a correct and valid method for calculating the system harmonics, and this method can also be extended to evaluate harmonics for other phase-control power supplies.

6. Conclusions

First, this paper introduced the principle of the ITER PF converter and its operation characteristics. Considering the features of the PF converter, the relationship between the input and output currents was deduced. Next, the piecewise method was presented to be applied to calculate the harmonics instead of integral operation. The harmonics calculation was simplified with the PF converter operation modes. A simulation model was established, and FFT analysis was presented to compare with the theoretical calculation. The simulation results were in accordance with the theoretical calculation. Finally, a similar experiment was carried out. The experimental results were consistent with the theoretical values and simulation analysis. The piecewise method was verified by these comparative analyses and so it can provide comparatively accurate values. The method is practical for calculating system harmonics. It can provide the references for the phase-control power supply.

The theoretical analysis was based on a comparatively ideal conditions; AC pulse in DC output current, asymmetric firing angle, asymmetric line voltage and some other reasons may cause non-characteristic harmonics. Although non-characteristic harmonics are much lower than characteristic harmonics, it may cause coupling effects with other equipment in a power grid. In the future, more attention needs to be paid to system transient harmonics analysis.

Acknowledgments

The authors would like to express gratitude to their colleagues in Institute of Plasma Physics, Chinese Academy of Sciences (ASIPP) for helpful discussions and suggestions. The views and opinions expressed herein do not necessarily reflect those of the ITER organization.

References

[1] Tao J *et al* 2011 ITER coil power supply and distribution system *Proc. IEEE/NPSS 24th Symp. on Fusion Engineering* (Chicago, IL: IEEE)
[2] Fu P *et al* 2013 *Fusion Sci. Technol.* **64** 741
[3] Song Z Q *et al* 2016 *IEEE Trans. Plasma Sci.* **44** 1677
[4] Sheng Z C, Xu L W and Fu P 2012 *Plasma Sci. Technol.* **14** 338
[5] Yang W *et al* 2009 *Plasma Sci. Technol.* **11** 493
[6] Task Force on Harmonics Modeling and Simulation, IEEE PES Harmonic Working Group 2001 *IEEE Trans. Power Deliv.* **16** 791
[7] Singh G K 2009 *Eur. Trans. Electr. Power* **19** 151
[8] Arrillaga J, Bradley D A and Bodger P S 1985 *Power System Harmonics* (New York: Wiley)
[9] Fukuda S, Ohta M and Iwaji Y 2008 *IEEE Trans. Power Electron.* **23** 1270
[10] Rice D E 1994 *IEEE Trans. Ind. Appl.* **30** 294
[11] Xu W 2003 Status and future directions of power system harmonic analysis *IEEE Power Engineering Society General Meeting* (Toronto: IEEE)
[12] Biringer P P and Slonim M A 1980 *IEEE Trans. Ind. Appl.* **IA-16** 242
[13] Slonim M A and Biringer P P 1980 *IEEE Trans. Ind. Appl.* **IA-16** 248
[14] Tooth D J, Finney S J and Williams B 2001 *IEEE Trans. Aerosp. Electron. Syst.* **37** 109
[15] Yuan H W *et al* 2014 *J. Fusion Energy* **33** 269
[16] Yuan H W *et al* 2014 Study on the four quadrants operation of ITER poloidal field converter system *IEEE Int. Power Electronics and Application Conf. and Exposition* (Shanghai: IEEE)
[17] Yuan H W *et al* 2014 *Plasma Sci. Technol.* **16** 1147